EUKARYOTIC CELL, Aug. 2010, p. 1184–1192 Vol. 9, No. 8
1535-9778/10/$12.00 doi:10.1128/EC.00006-10

C Terminus of Nce102 Determines the Structure and Function of Microdomains in the *Saccharomyces cerevisiae* Plasma Membrane▽

Martin Loibl,[1]† Guido Grossmann,[1]‡ Vendula Stradalova,[2] Andreas Klingl,[3] Reinhard Rachel,[3] Widmar Tanner,[1] Jan Malinsky,[1]* and Miroslava Opekarová[4]

Institute of Cell Biology and Plant Physiology, University of Regensburg, Regensburg, Germany[1]; Institute of Experimental Medicine, Academy of Sciences of the Czech Republic, Prague, Czech Republic[2]; Center for Electron Microscopy—NWF III, University of Regensburg, Regensburg, Germany[3]; and Institute of Microbiology, Academy of Sciences of the Czech Republic, Prague, Czech Republic[4]

Received 8 January 2010/Accepted 21 June 2010

The plasma membrane of the yeast *Saccharomyces cerevisiae* contains stably distributed lateral domains of specific composition and structure, termed MCC (membrane compartment of arginine permease Can1). Accumulation of Can1 and other specific proton symporters within MCC is known to regulate the turnover of these transporters and is controlled by the presence of another MCC protein, Nce102. We show that in an *NCE102* deletion strain the function of Nce102 in directing the specific permeases into MCC can be complemented by overexpression of the *NCE102* close homolog *FHN1* (the previously uncharacterized *YGR131W*) as well as by distant *Schizosaccharomyces pombe* homolog *fhn1* (*SPBC1685.13*). We conclude that this mechanism of plasma membrane organization is conserved through the phylum *Ascomycota*. We used a hemagglutinin (HA)/Suc2/His4C reporter to determine the membrane topology of Nce102. In contrast to predictions, its N and C termini are oriented toward the cytosol. Deletion of the C terminus or even of its last 6 amino acids does not disturb protein trafficking, but it seriously affects the formation of MCC. We show that the C-terminal part of the Nce102 protein is necessary for localization of both Nce102 itself and Can1 to MCC and also for the formation of furrow-like membrane invaginations, the characteristic ultrastructural feature of MCC domains.

Stable lateral domains coexist within the plasma membrane of the yeast *Saccharomyces cerevisiae*. Nce102, a protein originally thought to be involved in nonclassical export (6) and more recently in sensing sphingolipids (10), is the main organizer of one type of these domains, termed MCC (membrane compartment of Can1) (25). MCC consists of evenly distributed, isolated patches enriched in sterols and specific proteins (15, 16, 25, 26). We showed that MCC-specific proton symporters accumulate in these patches in a reversible, membrane potential-dependent manner. This Nce102-mediated transient MCC accumulation plays a key role in the turnover of the transporters (16). Each MCC patch is accompanied by an eisosome, a cytosolic complex located directly beneath the membrane (36).

In an early freeze-etching study, Moor and Mühlethaler (28) demonstrated that the yeast plasma membrane contains numerous furrow-like invaginations. Recently, MCC patches were identified with these plasma membrane structures, and Nce102 was shown to be necessary for furrow formation. On the ultrastructural level, the MCC patches of *nce102*Δ cells appeared as flat, smooth, elongated areas within an otherwise particle-rich plasma membrane (32).

There is now increasing evidence that cytosolic Pil1, a primary component of eisosomes, is a prerequisite for MCC patch formation. It marks the sites where Nce102 and the MCC-specific transporters will subsequently accumulate (16, 23, 29). Data published so far do not indicate a direct involvement of cytoskeletal components in this process (26). Accordingly, markers of classical endocytosis, which are coupled to the cortical patches of actin, were localized outside the MCC (16).

In this paper we examine the contribution of Nce102 to the organization of MCC patches and of furrow-like invaginations. Our results indicate that, in contrast to the prediction of four transmembrane domains (TMDs), the Nce102 molecule might span the plasma membrane only twice, the C and N termini being oriented toward the cytoplasm. We find that the C-terminal 6 amino acids of Nce102 are essential for MCC patch formation as well as for the formation of the furrow-like membrane invaginations. In addition it is shown that this Nce102 function is phylogenetically conserved among *Ascomycota*.

MATERIALS AND METHODS

Yeast strains and growth conditions. Yeast strains used in this study are listed in Table 1 (4, 15, 19, 33). If not stated otherwise, cells were grown in a rich medium (YPD [1% yeast extract, 2% peptone, 2% glucose]) at 30°C on a shaker. Synthetic defined (SD) medium contained 0.67% Difco yeast nitrogen base without amino acids and 2% glucose supplemented with, depending on which marker was used to select for transformed cells, uracil and adenine (both 20 μg/ml) and amino acids (histidine, methionine, and tryptophan, each at 20 μg/ml, and lysine and leucine, each at 30 μg/ml). All yeast transformations were carried out by the high-efficiency method described by Gietz and Woods (14).

Construction of overexpression and tagging plasmids. *S. cerevisiae* genes *NCE102* and *FHN1* (*YGR131W*) and *S. pombe* gene *fhn1* (*SPBC1685.13*) were amplified by PCR from genomic DNA using the following primers (F and R for forward and reverse, respectively): *NCE102*-F (ATATAAGCTTATAATGCTAGC CCTAGC), *NCE102*-R (ATTACTCGAGACTTGGGAAATGGTT), *FHN1*-F (A

* Corresponding author. Mailing address: Institute of Experimental Medicine, Academy of Sciences of the Czech Republic, Videnska 1083, 142 20 Prague, Czech Republic. Phone and fax: 420 241 062 597. E-mail: malinsky@biomed.cas.cz.

† Present address: Heidelberg Institute for Plant Science, Heidelberg University, Heidelberg, Germany.

‡ Present address: Carnegie Institution for Science, Department for Plant Biology, 260 Panama Street, Stanford, CA 94305.

▽ Published ahead of print on 25 June 2010.

TABLE 1. Yeast strains used in this study

Strain	Genotype	Reference or source
BY4741	*MAT***a** *his3Δ1 leu2Δ0 met15Δ0 ura3Δ0*	4
GYS90	BY4741; YIplac211-*CAN1-GFP*	15
GYS91	BY4741; *nce102*::*kanMX4*	EUROSCARF
VSY1	GYS91; *CAN1*::*GFP*::*LEU2* (YIp128)	This study
VSY4	VSY1; pVT100U-*NCE102-mRFP*	This study
VSY5	VSY1; pVT100U-*YGR131W-mRFP*	This study
VSY6	VSY1; pVT100U-*mRFP*	This study
VSY47	VSY1; pVT100U-*SPBC1685.13-mRFP*	This study
STY50	*MAT***a** *his4-401 leu2-3,112 trp1-1 ura3-52 HOL1-1 suc2*::*LEU2*	33
MLY95	STY50 pJK90	18
MLY90	STY50 pJK90-*NCE102*(1-519 bp)	This study
MLY91	STY50 pJK90-*NCE102*(1-438 bp)	This study
MLY92	STY50 pJK90-*NCE102*(1-282 bp)	This study
MLY93	STY50 pJK90-*NCE102*(1-189 bp)	This study
MLY94	STY50 pJK90-*NCE102*(1-84 bp)	This study
MLY100	BY4741; YIplac211-*NCE102*(1-438 bp)-*GFP*	This study
MLY46	BY4741; YIplac211-*NCE102-GFP*	This study
MLY105	GYS90; YIplac128-*NCE102*(1-438 bp)	This study
MLY106	GYS90; YIplac128-*NCE102*(1-501 bp)	This study

GCATCTAGAATAATAAATGCTATCAG), *FHN1*-R (AGTAGGATCCAACC TGGGAAATTGT), *S.pombe-fhn1*-F (CCCAAAGCTTATGGTTGGAATCAG), *S.pombe-fhn1*-R (AAAAGGATCCAACGGCAGACATGAC). Resulting fragments were cloned into plasmid pVT100U-mRFP, which was constructed as follows. The monomeric red fluorescent protein (mRFP) gene including an upstream MluI restriction site, the linker region, the 3′ untranslated region (UTR), and a downstream MfeI site was amplified by PCR from pmRFPkanMX using the primers KM33 (ATATACGCGTTGGAGCAGGGGCGGGTGCCTCCTCCGAGGAC GTC; F) and JST86 (AAAAAACAATTGCAGGCATTTGCTCGGCAT; R). The PCR product was ligated as an MluI-MfeI fragment into pVT100U (2μm *URA3* Amp^R) (35) and transformed into *Escherichia coli* for amplification.

To express 3′-terminally truncated versions of *NCE102*, the genomic sequence was amplified using the primer ML23 (GTGTTTGTTACGCATGCAAGCTTG ATATCGAAATGCTAGCCCTAGCTGATAAC), ML47 (ATATGGATCCTT AAACACCGACTTGGCCAGTTC; $NCE102_{1\text{-}167}$), or ML48 (ATATGGATCC TTAGATCATGTTGAAAACAGACATC; $NCE102_{1\text{-}146}$). The PCR products were inserted as HindIII-BamHI fragments into integrative plasmids YIplac128 and YIplac211-GFP (13, 15). Linearization of these plasmids with BcuI within the *NCE102* gene targets integration in wild-type *S. cerevisiae.* In the case of YIplac128-$NCE102_{1\text{-}167}$ and YIplac128-$NCE102_{1\text{-}146}$, the cells were subsequently transformed using YIplac211-*CAN1-GFP* (15) linearized by BcuI.

Isolation of crude membranes. Early logarithmic cells (100 optical density at 600 nm [OD_{600}] units) were washed twice by 10 mM NaN_3/NaF buffer to block endocytosis and resuspended in ice-cold TNE-I buffer (50 mM Tris-HCl, pH 7.4, 150 mM NaCl, and 5 mM EDTA), supplemented with protease inhibitors (1 mM phenylmethylsulfonyl fluoride [PMSF], 4 μM leupeptin, and 2 μM pepstatin). To isolate crude membranes, the cells were broken with glass beads in a FastPrep instrument (Thermo Fisher Scientific). Unbroken cells and larger cell debris were removed by two-step low-speed centrifugation (500 × *g* and 1,200 × *g*, 5 min each) in an Eppendorf centrifuge at 4°C. Crude membranes were pelleted at 20,000 × *g* for 75 min and resuspended in TNE-I buffer.

Cloning and analysis for topology determination. Topology analysis was performed as described by Kim et al. (18). To amplify and clone 3′-truncated versions of the *NCE102* gene into pJK90 (19), the following PCR primers were used (all primers contain a homologous region for *in vivo* ligation into pJK90): ML23 (F primer, see above) and R primers TGGTCTAGAGGTGTAACCACTTGAGTTC TTAGGGACTTGGGAAATGGTTGGAAC (ML24; amplification of all 519 bp of *NCE102*, excluding the stop codon), TGGTCTAGAGGTGTAACCACTTGAGT TCTTAGGGATCATGTTGAAAACAGACATC (ML25; amplification of 438 bp of *NCE102*), TGGTCTAGAGGTGTAACCACTTGAGTTCTTAGGTCTGATA CCAACGGCCAACAC (ML26; amplification of 282 bp of *NCE102*), TGGTCTA GAGGTGTAACCACTTGAGTTCTTAGGTTCAATGAAGTTGGCAAAGAC (ML27; amplification of 189 bp of *NCE102*), and TGGTCTAGAGGTGTAACCA CTTGAGTTCTTAGGTAACAACGAACTGATTAAACCG (ML28; amplification of 84 bp of *NCE102*). Genomic DNA was used as the template for PCR. For *in vivo* ligation, the vector pJK90 was linearized by digestion with SmaI and treated with calf intestinal alkaline phosphatase to prevent religation. *S. cerevisiae* strain STY50 was transformed with the linearized vector and the full-length *NCE102* or one of the shortened versions of *NCE102* and selected on SD plates lacking uracil (SD −ura plates). Plasmids were isolated, retransformed in *E. coli*, and sequenced. To monitor histidinol dehydrogenase activity, successfully transformed yeast cells were grown on selective media (SD −His −ura supplemented with 6 mM histidinol). For endo-β-*N*-acetylglucosaminidase H (Endo H) assays, 10% SDS and 10% β-mercaptoethanol were added to 20 μl of crude membranes (protein concentration, 8 to 12 μg/μl) to a final concentration of 0.5% each. After incubation at 45°C for 10 min, 88 μl of 100 mM sodium citrate buffer, pH 5.5, and 5.5 μl of 10% octylglucoside were added. The sample was split into two and incubated at 37°C either with 1 μl Endo H (gift from Ludwig Lehle, Regensburg, Germany) or with H_2O as a control. After 2 h of incubation, 1 μl of Endo H or water, respectively, was added again, and the incubation continued for another 2 h. After centrifugation (20,000 × *g* for 5 min), the supernatant was analyzed by SDS-PAGE.

Confocal microscopy. Living yeast cells cultured in SD medium (see Fig. 1 and 3) (log phase; OD_{600} of 0.5 to 1.0) were immobilized by a thin film of 1% agarose in SD medium and observed. Cells cultured in YPD (see Fig. 4) (overnight cultures) were washed briefly in 50 mM potassium phosphate buffer (pH 6.3; KPi), immobilized by a thin film of 1% agarose in KPi, and observed. Specimens were viewed using an LSM510-META confocal microscope (Carl Zeiss) with a 100× PlanApochromat oil immersion objective (numerical aperture [NA] = 1.4). Fluorescence signals of green fluorescent protein (GFP) and mRFP (excitation, 488 nm [Ar laser] and 561 nm [diode-pumped solid-state laser] [see Fig. 1] or 543 nm [He-Ne laser] [see Fig. 4]) were detected using band-pass 505- to 550-nm and long-pass 580-nm emission filters. In double-labeling experiments, sequential scanning was used to avoid any cross talk of fluorescence channels.

Preparation of freeze fracture replicas and electron microscopy. Cells from overnight culture were harvested by mild centrifugation (1,500 × *g* for 1 min) and washed in KPi buffer (pH 5.5). A 2-μl aliquot of the concentrated cell suspension was loaded onto a gold carrier and rapidly frozen in liquid nitrogen. The sample was cut with a cold knife (≤−185°C), etched for 4 min (−97°C; pressure ≤ 1.3×10^{-5} Pa) in a CFE-50 freeze-etch unit (Cressington, Watford, United Kingdom), shadowed (1 nm Pt/C, 45°; 10 nm C, 90°), and cleaned in fresh 70% H_2SO_4 for 16 h (30). Freeze fracture micrographs (see Fig. 5) were acquired using a cooled slow-scan charge-coupled device (CCD) camera (Tvips; Tietz, Gauting, Münich, Germany) mounted on a Philips CM 12 transmission electron microscope (FEI, Netherlands) operated at 120 kV.

RESULTS

Nce102 homologs share Nce102 function in plasma membrane organization. Phylogenetically, furrow-like invaginations of the yeast plasma membrane represent a highly conserved structure (reviewed by Stradalova et al. [32]). Proteins sharing a significant homology with Nce102, a protein shown to be necessary for the final step of the formation of furrows as well as of MCC patches in *S. cerevisiae*, are found in various species of *Ascomycota*. BLAST (Basic Local Alignment Search Tool) analysis (2) reveals more than 40 different Nce102 orthologs. We tested whether the molecular function of promoting the localization of specific transporters in the MCC/furrows is conserved among these Nce102-like proteins.

In the genome of *S. cerevisiae*, open reading frame (ORF) *YGR131W* codes for one of the closest Nce102 homologs (Fig. 1A). Ygr131w shows 55% identity (68% similarity) to Nce102, and its overexpression complements the Nce102 deletion. In the plasma membrane of the *nce102*Δ strain, Can1-GFP is distributed homogenously (16). When overexpressed in *nce102*Δ cells, Ygr131w-mRFP not only accumulates in MCC patches (16) but also induces the accumulation of Can1-GFP in this plasma membrane compartment. Due to the ability of *YGR131W* to replace this *NCE102* function, we named the gene *FHN1* (functional homolog of *NCE102*) (Fig. 1B to D). Since *FHN1* is not able to compensate for the *NCE102* dele-

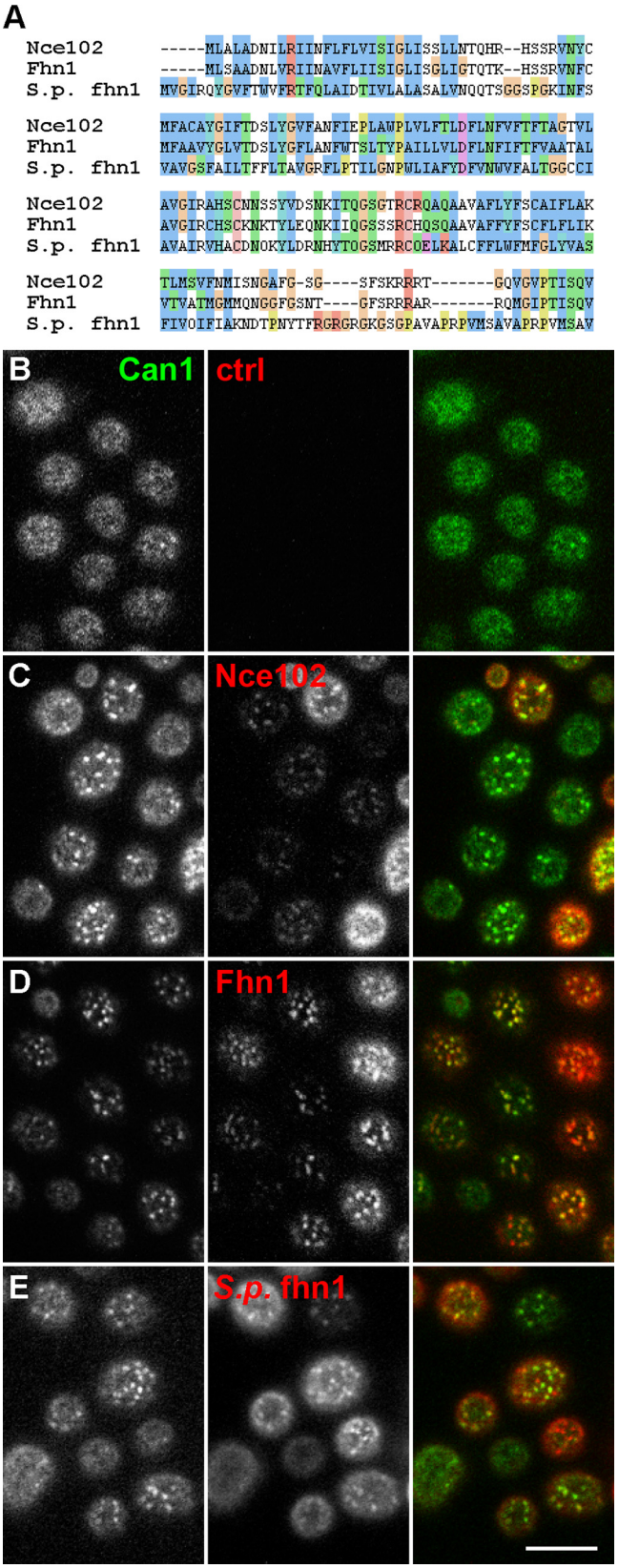

FIG. 1. Nce102-like proteins induce the accumulation of Can1 in MCC patches. (A) *S. cerevisiae* proteins Nce102 and Fhn1 (product of *YGR131W*) and *Schizosaccharomyces pombe* protein fhn1 were aligned using ClustalW 2.0 (22). In the *nce102*Δ mutant of *S. cerevisiae*, Can1-GFP was coexpressed either with an empty plasmid (B) or with vectors coding for *S. cerevisiae* Nce102-mRFP (C) and Fhn1-mRFP (D) and *S. pombe* fhn1-mRFP (E). Note the homogenous distribution of Can1-GFP in panel B and its focal appearance in panels C to E. Bar, 5 μm.

tion when expressed under the control of its own promoter, we conclude that its inherent expression level is not sufficient.

The replacement of Nce102 function in the plasma membrane organization could also be observed when a heterologous *NCE102*-like gene of *Schizosaccharomyces pombe*, the uncharacterized ORF *SPBC1685.13* (31% identity and 52% similarity to *S. cerevisiae NCE102*) (Fig. 1A) was expressed in the *S. cerevisiae nce102*Δ mutant (Fig. 1E). Similarly to Fhn1, the gene product of *SPBC1685.13* was targeted to MCC and induced significant accumulation of Can1-GFP in this compartment. Therefore, we named the gene *fhn1* (functional homolog of *S. cerevisiae NCE102*). Even though the primary structure of Fhn1 shows a relatively low degree of homology with Nce102 (see alignment of *NCE102*, *FHN1*, and *fhn1*), it complements the Nce102 deletion. We concluded therefore that the function of Nce102 in plasma membrane organization is probably widely conserved throughout *Ascomycota*.

Membrane topology of Nce102. Large conserved parts of Nce102 correspond to highly hydrophobic regions of the protein molecule. According to hydropathy analysis tools (e.g., TMHMM2.0; http://www.cbs.dtu.dk/services/TMHMM-2.0/) (21), the protein is predicted to possess 4 transmembrane helices, with N and C termini oriented toward the lumen of the endoplasmic reticulum (ER) during protein synthesis (Fig. 2A, model I) and outside the cell once it reaches the plasma membrane.

To determine the topology of Nce102 experimentally, we employed a technology of a hemagglutinin (HA)/Suc2/His4C chimeric protein tag as a topology reporter (7, 18), a technique widely used for membrane protein topology determination. We constructed vectors coding for Nce102 C-terminally truncated after the 1st, 2nd, 3rd, or 4th predicted transmembrane domain (at amino acid L28, E63, R94, or I146, respectively) (Fig. 2A, model I). The full-length Nce102 and the individual truncated versions described above were C-terminally tagged with HA/Suc2/His4C and expressed in an auxotrophic *his4* strain (7, 9, 18). The ability of the histidinol dehydrogenase (His4C) to convert histidinol to histidine enables a histidine-auxotrophic strain with the reporter located in the cytosol to grow on media lacking histidine but supplemented with histidinol. Invertase (Suc2) and His4C contain eight and four, respectively, consensus acceptor sites for N-linked glycosylation that could be glycosylated only if the reporter is translocated to the lumen of the endoplasmic reticulum. The HA tag is included to allow identification of the expressed fusion proteins by Western blotting.

Anti-HA antibody detected the fusion proteins in crude membranes prepared from all five strains, each expressing one of the truncated versions of *NCE102* or the full-length *NCE102* fused to the reporter. The shift to higher molecular masses of the fusion proteins containing amino acids 1 to 28, 1 to 63, and 1 to 94, which can be abolished by Endo H treatment, proved their glycosylation (Fig. 2C). Therefore, the C termini of these

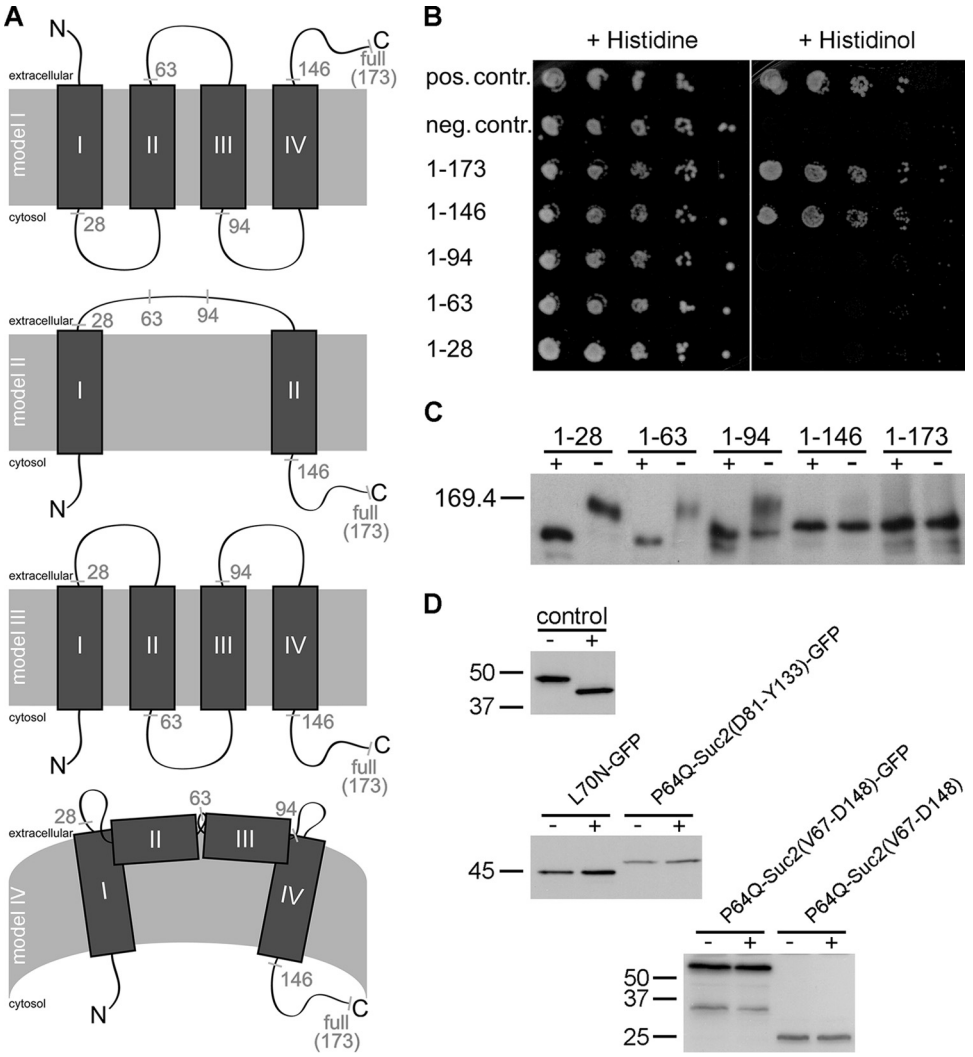

FIG. 2. Nce102 topology. (A) Predicted (I) and experimentally determined (II, III, and IV) topology alternatives for the Nce102 molecule. Sites used for the synthesis of Nce102 truncated versions are depicted. (B) Growth of *his4*Δ cells expressing truncated Nce102s fused to the HA/Suc2/His4C reporter construct was tested on histidine (control; left) and histidinol (His4 substrate; right). Positive control, pJK90-*OST4*-HA-*SUC2-HIS4C* (19); negative control, empty vector. (C) Glycosylation of the reporter can occur only if it faces the ER lumen. Total membrane fractions from strains expressing fusion proteins as described in Materials and Methods were either treated (+) or not treated (−) with Endo H. After SDS-PAGE and Western blotting, the fusion proteins were detected by anti-HA antibody. Cleavage of N-linked glycans was manifested by a shift of the molecular mass. (D) Glycosylation status of Nce102 tested with the use of shortened topology reporters. The positive control (Wbp1, top), L70N Nce102 mutant (middle, left lanes), and Nce102 molecules with shortened Suc2 fragments (middle, right lanes, and bottom) were compared (see text for details).

three constructs were exposed to the ER lumen during their biosynthesis, and consequently, in the plasma membrane, amino acids 28, 63, and 94 should be oriented outside the cell. No molecular mass shift or effect of Endo H treatment was detected in strains bearing the full-length (amino acids 1 to 173) version or the version consisting of amino acids 1 to 146, indicating thus that the stretch of amino acids 146 to 173 was oriented to the cytoplasm (Fig. 2C). This conclusion was also confirmed by the growth on histidinol of the histidine-auxotrophic strains bearing fusion constructs with the full-length or truncated (1 to 146) protein, indicating the cytoplasmic orientation of the C terminus (Fig. 2B).

These results indicate that the Nce102 protein contains only two transmembrane helices (Fig. 2A, model II), corresponding to the first (N-terminal) and last hydrophobic regions in the Nce102 molecule. The middle large hydrophobic region in this interpretation does not span the membrane. A precaution has to be taken is to consider the possibility that the bulky (125-kDa) topology reporter attached to this small (19-kDa) protein and its even smaller fragments could interfere with both their trafficking and folding. However, as shown in Fig. 3, at least the largest Nce102-derived chimeras are targeted properly to the plasma membrane. To minimize the danger of artificial misfolding, we further checked the Nce102 topology by inserting a shortened Suc2 fragment, D81 to Y133 or V67 to D148, into the intact protein. They were inserted after P64Q; including short additional amino acid stretches was thought to possibly prevent potential interference with the putative TMD 2. In

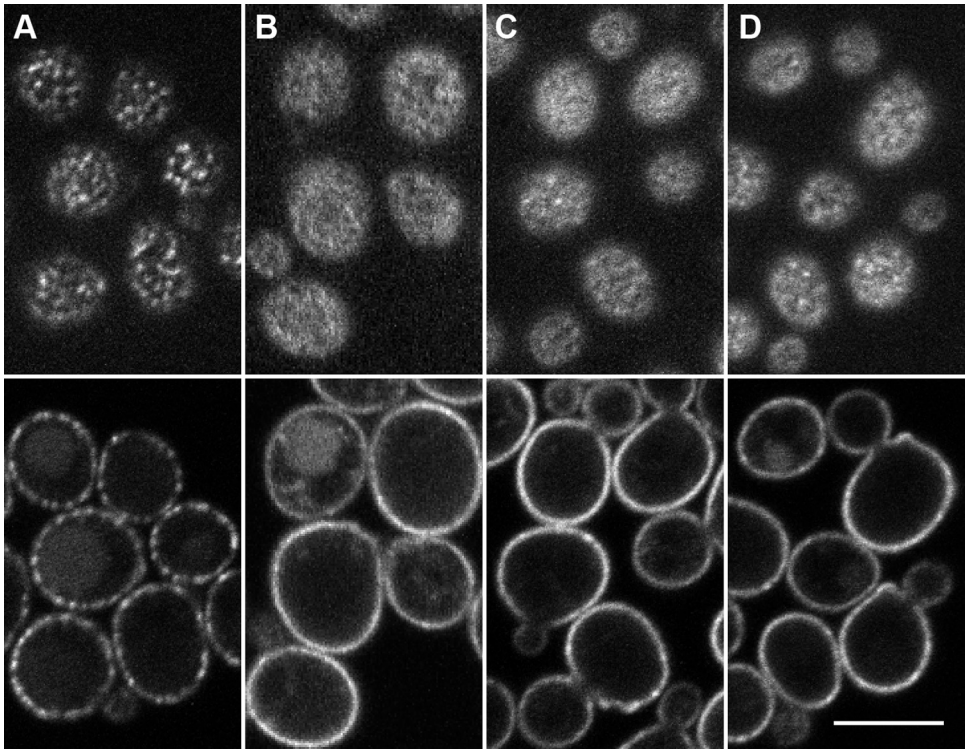

FIG. 3. The C-terminally truncated version of Nce102 is unable to sequester Can1 into MCC. Plasma membrane distributions of Can1-GFP in the wild type (A) and *NCE102* deletion mutant (B) were compared to that in the cells expressing the C-terminally truncated versions of Nce102, $Nce102_{1-146}$ (C) and $Nce102_{1-167}$ (D), under the control of the natural promoter. Surface confocal sections and central confocal cross sections are presented. Bar, 5 μm.

another construct, L70 in Nce102 was exchanged for N to generate a glycosylation site within the loop exposed to the ER lumen in both the computer-predicted topology (model I) and the Suc2/His4C-based experimentally assessed topology above (model II; in this case, however, the orientation of the whole molecule is inverted [Fig. 2A]). The proteins were immunodetected with specific anti-Nce102 antibody. ER protein Wbp1 was used as a positive control for Endo H digestion. As shown in Fig. 2D, the Endo H digestion was not accompanied by a shift in molecular weight with either of the tested proteins, while a clear shift was detected in the control (Wbp1). These results show that the Suc2 reporter was not glycosylated in the ER lumen. The putative model of 4 TMDs with N and C termini inside the cell has, therefore, not definitely been excluded, and model III of Fig. 2A has still to be considered as possibly correct.

The C terminus of Nce102 is necessary to target MCC-specific transporters into MCC. Besides the hydrophobic regions, also the C terminus is highly conserved among the Nce102 homologs. We tested the physiological significance of this highly conserved C terminus in targeting Nce102 to MCC and/or in the gathering (concentrating) of other MCC residents.

The total C-terminal part following the last predicted transmembrane helix, consisting of 27 amino acids, was removed from Nce102, and this truncated version ($Nce102_{1-146}$) was expressed in a wild-type background under the control of an endogenous promoter. In the resulting strain, Can1-GFP was

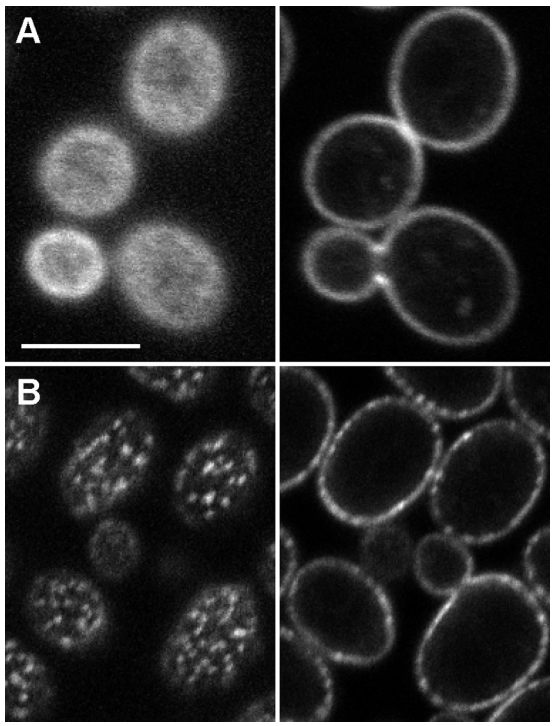

FIG. 4. The C-terminally truncated Nce102 does not localize to MCC. The plasma membrane distribution of C-terminally truncated $Nce102_{1-146}$ (A) tagged with GFP and that of the full-length Nce102-GFP (B) are shown on surface confocal sections (left) and central confocal cross sections (right). Note the absence of a characteristic MCC pattern in panel A. Bar, 5 μm.

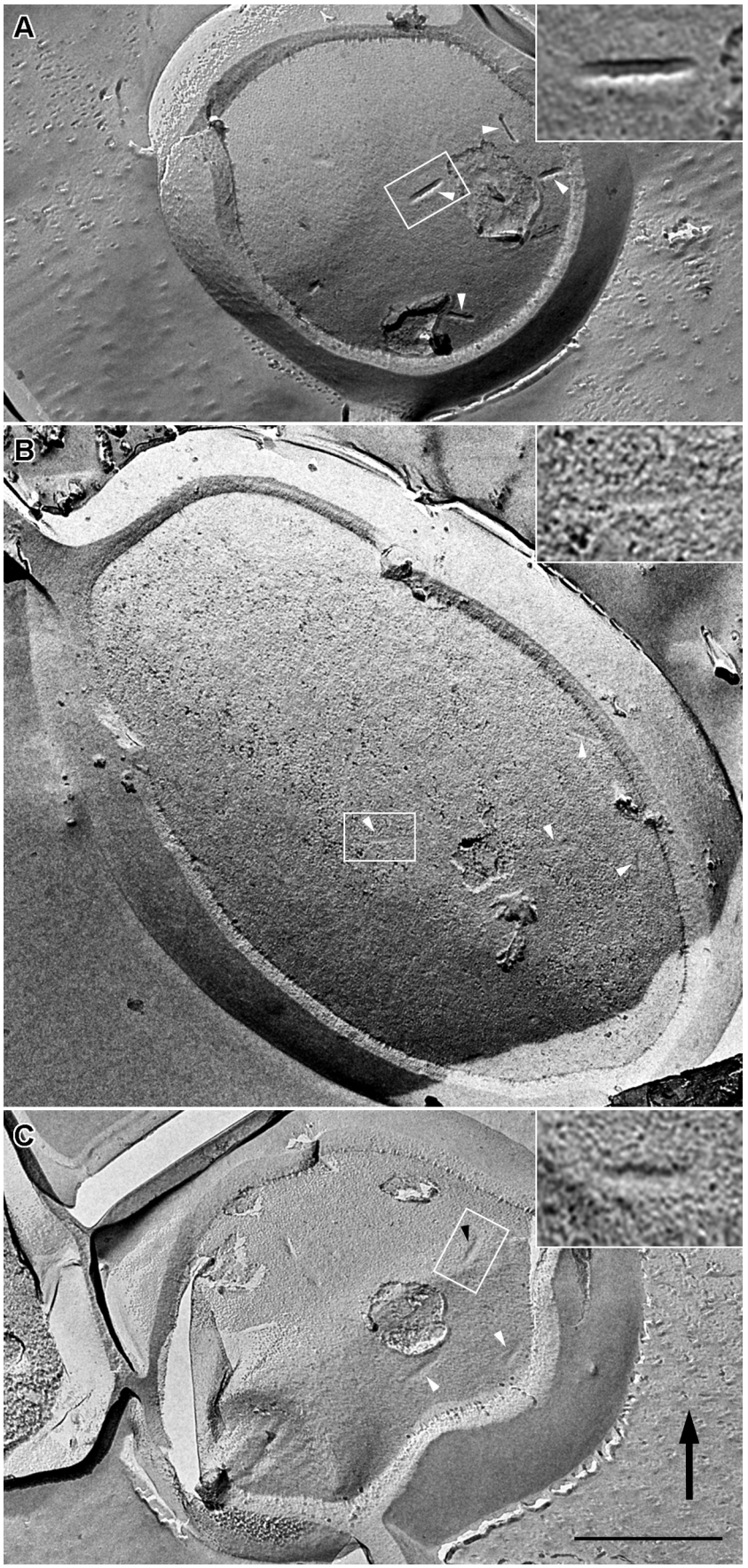
A
B
C

distributed homogenously as in the *nce102*Δ background, which means that Nce102$_{1–146}$ did not substitute for the Can1 accumulation-related function of Nce102 (Fig. 3A to C). A deletion of the 6 terminal amino acids only (Nce102$_{1–167}$) resulted in an identical effect (Fig. 3D). Expression levels of the full-length protein and its C-terminally truncated proteins were mutually comparable (data not shown). As shown by localization of GFP fusion proteins, the two truncated Nce102 versions reached the plasma membrane but, in contrast to the full-length molecule, were distributed homogenously (Fig. 4). These results document that the stretch of the very last 6 amino acids of Nce102 is responsible for directing this protein to MCC patches.

The C terminus of Nce102 is necessary for the formation of the plasma membrane invaginations. As previously observed in freeze-etch preparations of plasma membrane replicas, the full deletion of *NCE102* results in a lack of furrow-like invaginations (32). We therefore tested whether the C-terminal truncation of the Nce102 protein has a similar effect. For direct comparability with the results obtained by confocal microscopy we used the strains expressing *NCE102*-GFP and *NCE102*$_{1–146}$-GFP for replica preparation. In total, 111 cells expressing full-length *NCE102*-GFP and 33 cells expressing *NCE102*$_{1–146}$-GFP were analyzed. While all cells expressing the full-length *NCE102* gene formed furrows, only in 3 out of 33 analyzed Nce102$_{1–146}$-containing cells could shallow, premature furrow-like invaginations be identified. The remaining 90% of cells exhibited flat plasma membranes devoid of the typical furrow-like invagination pattern. Flat, smooth, elongated areas with surface densities comparable to that observed in furrows of wild-type cells were detected instead (Fig. 5). This remarkable change in the plasma membrane morphology was virtually identical to the phenotype previously observed for the *nce102*Δ strain (32). We conclude that, after its C-terminal part had been deleted, Nce102 lost its function in formation of furrows.

DISCUSSION

So far, we have documented nine proteins sharing the MCC localization: four members of the Sur7 family (Sur7, Ynl149c, Fmp45, and Ylr414c), three proton symporters (Can1, Fur4, and Tat2), and Nce102, with its close homolog Fhn1 (15, 16, 25, 26). Among those, no general MCC targeting sequence was revealed. Our findings rather support a step-by-step mechanism for MCC formation as suggested previously: (i) Pil1-driven assembly of planar membrane domains (primary MCC patches) containing Sur7 family proteins; (ii) recruitment of specific lipids, Nce102, and transporters into these domains; and (iii) lipid- and/or protein-mediated invagination of the MCC membrane (for details see references 27 and 32). Previously we showed that Nce102 directs the proton transporters into MCC patches, where they are protected against untimely turnover (16). In this study we document that the mechanism of plasma membrane domain formation and this MCC function is probably conserved through the largest phylum of fungi, the *Ascomycota*. This conclusion is based on the observation that, by expressing one of the most distant Nce102 homologs coded by *S. pombe fhn1*, we were able to reconstitute the Can1-enriched MCC patches in the *nce102*Δ strain of *S. cerevisiae*.

The hydropathy plot of Nce102 revealed four potential membrane-spanning domains. This prediction of the membrane topology, however, does not seem to be correct, at least in the sense of the protein orientation. Using a combination of glycosylation and growth assays, we determined that the C terminus of Nce102 is oriented toward the cytoplasm, while in the predicted protein structure it is exposed to the cell exterior. Taking this observation into account, we consider three putative models of Nce102 accommodation in the plasma membrane (Fig. 2A, models II to IV). The first one (model II), assuming that the protein crosses the membrane only twice, is based on a set of experiments where the topology was determined using the entire HA/Suc2/His4C reporter. However, this tag is quite bulky (125 kDa) compared to the tested Nce102 fragments, and thus it is possible that, during the membrane insertion, the fusion proteins do not fold correctly. On the other hand, it is worthwhile mentioning that, using the same strategy as that described above, we confirmed unambiguously the tetraspan topology of another protein residing in MCC, Sur7 (20; V. Stradalova, unpublished results). To obviate the interference of the bulky HA/Suc2/His4C reporter with the membrane insertion of Nce102-derived peptides, much smaller Suc2 fragments (6 and 9.3 kDa) were tested as glycosylation reporters. As evident from Fig. 2D, in this case the C-terminal reporter on fragment Nce102$_{1-63}$ is not glycosylated, which indicates that the hydrophilic loop following amino acid 63 is not exposed to the ER lumen and therefore probably faces the cytoplasm when the Nce102 protein is incorporated into the plasma membrane. The same holds for a newly created glycosylation site generated at amino acid 70. Conclusions from these results are summarized in topology model III in Fig. 2A. Neither of the two models, however, might be fully fitting. It is noteworthy that the first predicted TMD in Nce102 consists of 18 amino acids only. Usually, at least 23 amino acid residues are required for spanning the yeast plasma membrane (31, 37). However, 7 of 10 amino acid residues of the cytoplasmic N terminus are of positive hydropathy index, and the possibility that they might be involved in protein embedding cannot be excluded. The first extracellular stretch in model III consists of 12 highly polar amino acids, while the second loop, the internal one, contains only 9 amino acids, 7 of which are nonpolar. The other two amino acids are prolines, which are well documented to influence the conformation of, e.g., helical regions (1, 24, 39). Helices containing proline have a pronounced kink, with

FIG. 5. The C-terminally truncated version of Nce102 is unable to form furrow-like invaginations of the plasma membrane. The fine structures of the plasma membrane in wild-type (A)- and C-terminally truncated Nce102$_{1–146}$-expressing cells (B and C) were compared on freeze-etched replicas. MCC domains were marked (arrowheads). Instead of invaginations (A), a flat membrane was found in cells containing the incomplete Nce102 protein (B). Frequently, smooth, elongated areas could be detected in the membrane surface (insert in panel B). Only occasionally could shallow invaginations be recognized, too (C). Regions magnified in inserts are highlighted by frames. Bar, 1 μm.

bending of the helical axis of approximately 30° away from the side with the proline residue (38). Regarding all our results and the specific features of Nce102, we suggest topology model IV, where the proposed TMDs 2 and 3 do not span the plasma membrane but are inserted into the outer leaflet of the membrane. Due to its high hydrophobicity, the short 9-amino-acid stretch located between potential TMDs 2 and 3 might be incorporated into the lipid bilayer as well. In this case, the whole stretch of amino acids 40 to 95 could be embedded in the plasma membrane and the presence of the prolines might be involved in bending this helix.

It is plausible to speculate that these specific features of the Nce102 primary structure endow Nce102 with a certain topological flexibility, which might be of physiological relevance. In this context it is interesting to refer to the recent studies of Fröhlich et al. (10), where Nce102 has been proposed to act as a sensor for sphingolipids, regulating the appearance of the MCC pattern via phosphorylation of Pil1, a cytosolic protein accumulated beneath the MCC patches. Indeed, the involvement of Nce102 in processes including changes of the plasma membrane lipid composition is indicated by its increased expression reported in several screening studies looking for responses to environmental changes, like heat stress, oxidative and osmotic shocks, nitrogen source depletion, diauxic shift, transition to invasive growth, and introduction of various toxic substances (8, 11, 12, 34). The monitoring and transferring of signals from the environment may be due to changes in Nce102 topology, e.g., in the positioning of originally proposed TMDs 2 and 3. Our results document that the N and C termini of Nce102 face the cytosol, and we favor the possibility that the middle part of the molecule is incorporated in or tightly attached to the outer leaflet of the plasma membrane.

We identified a short C-terminal motif (PTISQV), the absence of which resulted in a loss of Nce102 function in the formation of MCC patches as well as of the plasma membrane invaginations (Fig. 3 to 5). Among the Nce102-like proteins resulting from our BLAST search, the motif is strongly (proline, 100% of 42 sequences analyzed; glutamine and valine, >95%) conserved in *Ascomycota* (data not shown). Our data show that even one of the most distant variants of this motif (PvmSaV [lowercase letters refer to amino acids not conserved in the *S. cerevisiae* version of the Nce102 protein]) in *S. pombe* Fhn1 is sufficient to accomplish the Nce102 function. Apparently, the C-terminal part of Nce102 is required for the local accumulation of the protein within Pil1-assembled domains (Fig. 4). In principle, two different mechanisms of membrane bending following this accumulation can be suggested. (i) The consequent transporter/sterol accumulation in MCC patches (15) promotes positive membrane curvature (32). Plasma membrane curvature caused by intercalation of ergosterol into the plane would play a key role in this case. However, lipids with high spontaneous curvature (like sterols) were shown to exhibit rather weak curvature preferences when inserted into membranes (17). (ii) It is possible that the central hydrophobic region of the Nce102 molecule is embedded into the outer layer of the plasma membrane (Fig. 2A, model IV). It is known that a shallow insertion of small hydrophobic inclusions effectively induces membrane curvatures (5). A critical amount of Nce102 at the patches could, in this case, induce the membrane bending. Many other proteins involved in the organization of membrane microdomains, for example, caveolins, reticulons, and flotillins (reggies), contain at least one membrane-integrated, but not membrane-spanning domain, which, it has been suggested, adopts a hairpin structure (3).

Based on our ultrastructural studies, we suggest that Nce102 operates also as a structural protein in bending the plasma membrane, which, of course, involves also the effects of specific lipids in the plasma membrane region. The role of Nce102 in specific structure formation does not exclude the possibility that Nce102 has additional functions.

ACKNOWLEDGMENTS

We are very grateful to Ingrid Fuchs for technical assistance. We also thank Katerina Malinska from the Institute of Experimental Botany, Academy of Sciences of the Czech Republic (Prague), for the construction of the pVTU100-mRFP plasmid and Sabine Strahl, University of Heidelberg, for technical advice.

V.S., M.O., and J.M. were financially supported by the Grant Agency of the Czech Republic (projects 204/07/0133, 204/08/J024, and 204/09/1924), the Grant Agency of the Academy of Sciences of the CR (KAN200520801), and by institutional grants (AVOZ50390703 and AV0Z50200510). M.L., G.G., W.T., A.K., and R.R. were supported by the Deutsche Forschungsgemeinschaft (DFG projects TA 36/18–1, TH, and SFB699 Z2). This work was also financially supported by the German Fonds der chemischen Industrie.

REFERENCES

1. **Altmann, K.-H., J. Wojcik, M. Vasquez, and H. A. Scheraga.** 1990. Helix-coil stability constants for the naturally occurring amino acids in water. XXIII. Proline parameters from random poly (hydroxybutylglutamine-co-L-proline). Biopolymers **30:**107–120.
2. **Altschul, S. F., W. Gish, W. Miller, E. W. Myers, and D. J. Lipman.** 1990. Basic local alignment search tool. J. Mol. Biol. **215:**403–410.
3. **Bauer, M., and L. Pelkmans.** 2006. A new paradigm for membrane-organizing and -shaping scaffolds. FEBS Lett. **580:**5559–5564.
4. **Brachmann, C. B., A. Davies, G. J. Cost, E. Caputo, J. Li, P. Hieter, and J. D. Boeke.** 1998. Designer deletion strains derived from Saccharomyces cerevisiae S288C: a useful set of strains and plasmids for PCR-mediated gene disruption and other applications. Yeast **14:**115–132.
5. **Campelo, F., H. T. McMahon, and M. M. Kozlov.** 2008. The hydrophobic insertion mechanism of membrane curvature generation by proteins. Biophys. J. **95:**2325–2339.
6. **Cleves, A. E., D. N. Cooper, S. H. Barondes, and R. B. Kelly.** 1996. A new pathway for protein export in *Saccharomyces cerevisiae*. J. Cell Biol. **133:** 1017–1026.
7. **Deak, P. M., and D. H. Wolf.** 2001. Membrane topology and function of Der3/Hrd1p as a ubiquitin-protein ligase (E3) involved in endoplasmic reticulum degradation. J. Biol. Chem. **276:**10663–10669.
8. **DeRisi, J. L., V. R. Iyer, and P.O. Brown.** 1997. Exploring the metabolic and genetic control of gene expression on a genomic scale. Science. **278:**680–686.
9. **Deshaies, R. J., and R. Schekman.** 1987. A yeast mutant defective at an early stage in import of secretory protein precursors into the endoplasmic reticulum. J. Cell Biol. **105:**633–645.
10. **Fröhlich, F., K. Moreira, P. S. Aguilar, N. C. Hubner, M. Mann, P. Walter, and T. C. Walther.** 2009. A genome-wide screen for genes affecting eisosomes reveals Nce102 function in sphingolipid signaling. J. Cell Biol. **185:** 1227–1242.
11. **Gasch, A. P., P. T. Spellnam, C. M. Kao, O. Carmel-Harel, M. B. Eisen, G. Storz, D. Botstein, and P. O. Brown.** 2000. Genomic expression programs in the response of yeast cells to environmental changes. Mol. Biol. Cell **11:** 4241–4257.
12. **Gasch, A. P., M. Huang, S. Metzner, D. Botstein, S. J. Elledge, and P. O. Brown.** 2001. Genomic expression responses to DNA-damaging agents and the regulatory role of the yeast ATR homolog Mec1p. Mol. Biol. Cell **12:**2987–3003.
13. **Gietz, R. D., and A. Sugino.** 1988. New yeast-Escherichia coli shuttle vectors constructed with in vitro mutagenized yeast genes lacking six-base pair restriction sites. Gene **74:**527–534.
14. **Gietz, R. D. and R. A. Woods.** 2002. Transformation of yeast by lithium acetate/single-stranded carrier DNA/polyethylene glycol method. Methods Enzymol. **350:**87–96.
15. **Grossmann, G., M. Opekarová, J. Malinsky, I. Weig-Meckl, and W. Tanner.** 2007. Membrane potential governs lateral segregation of plasma membrane proteins and lipids in yeast. EMBO J. **26:**1–8.
16. **Grossmann, G., J. Malinsky, W. Stahlschmidt, M. Loibl, I. Weig-Meckl,**

W. B. Frommer, M. Opekarová, and W. Tanner. 2008. Plasma membrane microdomains regulate turnover of transport proteins in yeast. J. Cell Biol. **183:**1075–1088.
17. **Kamal, M. M., D. Mills, M. Grzybek, and J. Howard.** 2009. Coupling between membrane curvature and lipid shape: measurement of the curvature preference of fluorescently labeled phospholipids. Proc. Natl. Acad. Sci. U. S. A. **106:**22245–22250.
18. **Kim, H., K. Melén, and G. von Heijne.** 2003. Topology models for 37 *Saccharomyces cerevisiae* membrane proteins based on C-terminal reporter fusions and predictions. J. Biol. Chem. **278:**10208–10213.
19. **Kim, H., Q. Yan, G. von Heijne, G. A. Caputo, and W. J. Lennarz.** 2003. Determination of the membrane topology of Ost4p and its subunit interactions in the oligosaccharyltransferase complex in *Saccharomyces cerevisiae*. Proc. Natl. Acad. Sci. U. S. A. **100:**7460–7464.
20. **Kim, H., K. Melén, M. Österberg, and G. von Heijne.** 2006. A global topology map of the *Saccharomyces cerevisiae* membrane proteome. Proc. Natl. Acad. Sci. U. S. A. **103:**11142–11147.
21. **Krogh, A., B. Larsson, G. von Heijne, and E. L. Sonnhammer.** 2001. Predicting transmembrane protein topology with a hidden Markov model: application to complete genomes. J. Mol. Biol. **305:**567–580.
22. **Larkin, M. A., G. Blackshields, N. P. Brown, R. Chenna, P. A. McGettigan, H. McWilliam, F. Valentin, I. M. Wallace, A. Wilm, R. Lopez, J. D. Thompson, T. J. Gibson, and D. G. Higgins.** 2007. Clustal W and Clustal X version 2.0. Bioinformatics **23:**2947–2948.
23. **Luo, G., A. Gruhler, Y. Liu, O. N. Jensen, and R. C. Dickson.** 2008. The sphingolipid long-chain base-Pkh1/2-Ypk1/2 signaling pathway regulates eisosome assembly and turnover. J. Biol. Chem. **283:**10433–10444.
24. **MacArthur, M. W., and J. M. Thornton.** 1991. Influence of proline residues on protein conformation. J. Mol. Biol. **218:**397–412.
25. **Malínská, K., J. Malinsky, M. Opekarová, and W. Tanner.** 2003. Visualization of protein compartmentation within the plasma membrane of living yeast cells. Mol. Biol. Cell **14:**4427–4436.
26. **Malínská, K., J. Malinsky, M. Opekarová, and W. Tanner.** 2004. Distribution of Can1p into stable domains reflects lateral protein segregation within the plasma membrane of living S. cerevisiae cells. J. Cell Sci. **117:**6031–6041.
27. **Malinsky, J., M. Opekarová, and W. Tanner.** 14 April 2010. The lateral compartmentation of the yeast plasma membrane. Yeast doi:10.1002/yea.1772.
28. **Moor, H., and K. Mühlethaler.** 1963. Fine structure in frozen-etched yeast cells. J. Cell Biol. **17:**609–628.
29. **Moreira, K. E., T. C. Walther, P. S. Aguilar, and P. Walter.** 2009. Pil1 controls eisosome biogenesis. Mol. Biol. Cell **20:**809–818.
30. **Rachel, R., I. Wyschkony, S. Riehl, and H. Huber.** 2002. The ultrastructure of *Ignicoccus*: evidence for a novel outer membrane and for intracellular vesicle budding in an archaeon. Archaea **1:**9–18.
31. **Rayner, J. C. and H. R. B. Pelham.** 1997. Transmembrane domain-dependent sorting of proteins to the ER and plasma membrane in yeast. EMBO J. **16:**1832–1841.
32. **Stradalova, V., W. Stahlschmidt, G. Grossmann, M. Blažíková, R. Rachel, W. Tanner, and J. Malinsky.** 2009. Furrow-like invaginations of the yeast plasma membrane correspond to membrane compartment of Can1 (MCC). J. Cell Sci. **122:**2887–2894.
33. **Strahl-Bolsinger, S., and A. Scheinost.** 1999. Transmembrane topology of Pmt1p, a member of an evolutionary conserved family of protein O-mannosyltransferases. J. Biol. Chem. **274:**9068–9075.
34. **Suzuki, C., Y. Hori, and Y. Kashiwagi.** 2003. Screening and characterization of transposon-insertion mutants in a pseudohyphal strain of Saccharomyces cerevisiae. Yeast **20:**407–415.
35. **Vernet, T., D. Dignard, and D.Y. Thomas.** 1987. A family of yeast expression vectors containing the phage f1 intergenic region. Gene **52:**225–233.
36. **Walther, T. C., J. H. Brickner, P. S. Aguilar, S. Bernales, C. Pantoja, and P. Walter.** 2006. Eisosomes mark static sites of endocytosis. Nature **439:**998–1003.
37. **Watson, R. T., and J. E. Pessin.** 2001. Transmembrane domain length determines intracellular membrane compartment localization of syntaxins 3, 4, and 5. Am. J. Physiol. Cell Physiol. **281:**C215–C223.
38. **Woolfson, D. N., and D. H. Williams.** 1990. The influence of proline residues on alpha-helical structure. FEBS Lett. **277:**185–188.
39. **Yun, R. H., A. Anderson, and J. Hermans.** 1991. Proline in alpha-helix: stability and conformation studied by dynamics simulation. Proteins **10:**219–228.